SCIENCE CHINA
Earth Sciences

SPECIAL TOPIC: GlobeLand30 remote sensing mapping innovation and large data analysis
• RESEARCH PAPER •

December 2016 Vol.59 No.12:2285–2294
doi: 10.1007/s11430-015-5277-0

Relationship between nitrogen deposition and LUCC and its impact on terrestrial ecosystem carbon budgets in China

LU XueHe[1,2], JIANG Hong[1,2*], ZHANG XiuYing[1,2] & JIN JiaXin[1,2]

[1] *Jiangsu Provincial Key Laboratory of Geographic Information Science and Technology, Nanjing University, Nanjing 210023, China;*
[2] *International Institute for Earth System Science, Nanjing University, Nanjing 210023, China*

Received April 14, 2016; accepted October 11, 2016; published online November 4, 2016

Abstract Increased nitrogen (N) deposition and land-use and land-cover change (LUCC) have influenced the terrestrial ecosystem carbon budget in China over the past few decades. However, the coupling effects of N deposition and LUCC on the carbon cycle remain unclear. This study first evaluated the effects of LUCC on N deposition based on estimated N deposition data from NO_2 column remote sensing data and the GlobeLand30 LUCC dataset, and then assessed the coupling effects of N deposition and LUCC on carbon budgets in China based on a terrestrial ecosystem process-based model. The results showed that the average rate of increase in N deposition in China was 0.35 Tg N yr^{-1} (Tg = 10^{12} g), which caused net primary production (NPP) and net ecosystem production (NEP) to rise by 92.2 Tg C yr^{-1} and 46.9 Tg C yr^{-1}, respectively. The effects of LUCC reduced N deposition by 0.21 Gg N yr^{-1} (Gg = 10^9 g). The land changed from forest to cropland had the greatest rate of increase in N deposition among all types of land-cover change. Changes from cropland to forest slowed the rate of N deposition increase the most. Generally, the change in N deposition resulting from LUCC reduced NPP and NEP by 0.7 and 0.4 Gg C yr^{-1}, respectively. Compared with the total effects of N deposition on NPP and NEP, N deposition changes caused by LUCC had a limited aggregate effect on the C budget.

Keywords Carbon budget, Nitrogen deposition, Land-use and land-cover change, Remote sensing, Model simulation

Citation: Lu X H, Jiang H, Zhang X Y, Jin J X. 2016. Relationship between nitrogen deposition and LUCC and its impact on terrestrial ecosystem carbon budgets in China. Science China Earth Sciences, 59: 2285–2294, doi: 10.1007/s11430-015-5277-0

1. Introduction

Carbon (C) assimilation is limited by insufficient soil N in many ecosystems (Luo et al., 2004; Zhang et al., 2014). Moreover, N limitation has become even more serious because of the effects of increasing atmospheric CO_2 concentration and climate change (Norby et al., 2010). Soil N content has been changed by atmospheric N deposition as a result of increased human activity since industrialization (Dentener et al., 2006), which has had further effects on global C budgets (Law, 2013). In China, this situation is more serious due to the rapid economic development. At the beginning of the 21st century, the national average N deposition rate was ~21.1 kg N ha^{-1} yr^{-1} (Liu et al., 2013), which has further increased nearly 59% in the past few decades (Lü and Tian, 2014). In some economically developed provinces, N deposition is even several times greater than the national average (Gu et al., 2012). The rapid increase of N deposition greatly affects ecosystem C budgets in China (Lü et al., 2012).

Changes in atmospheric N are connected with land-cover types. The rapidly increasing N deposition in China is related to the growth of surface nitric gas emissions from cropland and urban areas (Gu et al., 2013). In cropland, nitric gas emission is mainly N_4^+ from fertilizer application. Given its short transmission distance, N_4^+ usually deposits near the emission

* Corresponding author (email: jianghong_china@hotmail.com)

sources (Cornell et al., 2003). In urban areas, NO_3^- is mainly nitric gas emission from fossil fuel combustion during industrial production and traffic pollution. In contrast with N_4^+ in cropland, NO_3^- can affect wider areas because of its long-distance transmission in the atmosphere. In addition, land use affects boundary layer conditions, including surface roughness (Ouyang et al., 2003), moisture and heat flux (Seinfeld and Pandis, 2012), which are important to dry and wet N deposition.

Substantial land cover changes have been caused by the rapid economic development in China over the past 30 years. However, Chinese land use/land cover change (LUCC) policy since the 21st century has shifted from all-out exploitation to a balance between exploitation and conservation. Currently, the characteristics of Chinese LUCC are such that forest and urban areas are increasing while grasslands are shrinking and croplands remained unchanged (Liu et al., 2014). This rapid land-use change has already affected atmospheric N deposition patterns, which in turn affect C cycling in terrestrial ecosystems. Owing to a lack of necessary datasets such as long-term N deposition data and high spatial-resolution land-cover data, few studies have explored either the relationship between N deposition and land-cover change or how their relationship may affect the C budgets of terrestrial ecosystems. However, in recent years, these limitations have been surmounted by the new method of remote sensing to estimate N deposition and the availability of land-cover datasets with high spatial resolution. Therefore, this study evaluates the effects of N deposition changes arising from LUCC on terrestrial ecosystem C budgets, based on a terrestrial ecosystem model (IBIS).

2. Method and data

First, N deposition rates were estimated from NO_2 columns retrieved from 2000–2010 satellite data of China. Then, land-cover change was summarized by comparison between GlobeLand30 datasets from 2000 and 2010. After that, land-cover change and N deposition data were used to evaluate the influences of land-cover change on N deposition. Finally, simulated C-N coupling results of the terrestrial ecosystem model IBIS (Integrated Biosphere Simulator) were used to assess the effects of N deposition change caused by land-cover change on terrestrial ecosystem C budgets. Details about the method and data used in this study are introduced below.

2.1 Estimation of N deposition rates

Generally, regional N deposition is monitored using a network of observation stations, but temporal and spatial coverages are limited. In China, a national observation network for N deposition has not been established. Hence, long-term national data on N deposition remain scarce. Such deposition can be simulated by atmospheric chemical models, but this is not suitable for simulating high spatial-resolution, long-term deposition, because the simulation requires too much time. Therefore, no long-term N deposition datasets from atmospheric chemistry model simulations have been released until recently.

Remote sensing technology has recently made it possible to estimate N deposition rates, using space-based measurement of NO_2 columns. Studies have estimated N deposition from those columns as retrieved from satellite (Lu et al., 2013; Ma et al., 2012). Based on the method of Lu et al. (2013), multiple linear regression describes N deposition as a function of meteorological and NO_2 column data, as

$$N_{dep} = a_0 + a_1 t + a_2 p + a_3 h + a_4 w_e + a_5 w_n + a_6 c. \quad (1)$$

In this equation, a_0, a_1, a_2, a_3, a_4, a_5, a_6 represent regression coefficients of the linear regression; N_{dep} is atmospheric N deposition; t is surface temperature; p, h ,w_e, w_n and c represent precipitation, relative humidity, meridional wind speed, zonal wind speed and NO_2 column concentration, respectively.

To estimate N deposition within every grid cell in our study area, grid data of N deposition, NO_2 column concentration, and meteorological data are needed to calculate the coefficients a_i in eq. (1). N deposition data were from the atmospheric chemical model MOZART (Model for Ozone and Related Chemical Tracers) over 2007 to 2010. NO_2 column concentrations were retrieved from the Global Ozone Monitoring Experiment (GOME) and Ozone Monitoring Instrument (OMI). Meteorological data were downloaded from the China Meteorological Association's data sharing website (http://data.cma.cn/). All data were resampled to 0.25° spatial resolution by interpolation. Because of collinearity among multiple factors, principal component regression was used to eliminate this problem following the method of Lu et al. (2013).

Because there is no single satellite NO_2 column concentration data series that covers the entire study period (2000–2010), GOME and OMI data were both used. In eq. (1), the GOME NO_2 column was used from 2000 to 2004, and OMI NO_2 column data were used from 2005 to 2010. The gap between the two data series was smoothed by eq. (2).

$$V_{2010}^{\mathrm{OMI'}} = V_{2010}^{\mathrm{OMI}} \times \frac{\overline{V}_{2000\text{-}2004}^{\mathrm{GOME}}}{\overline{V}_{2005\text{-}2010}^{\mathrm{OMI}}}, \quad (2)$$

where $V_{2010}^{\mathrm{OMI'}}$ is the smoothed OMI NO_2 column concentration in 2010, V_{2010}^{OMI} is the original OMI NO_2 column concentration in that year, $\overline{V}_{2000\text{-}2004}^{\mathrm{GOME}}$ is the average GOME column concentration from 2000 to 2004, and $\overline{V}_{2005\text{-}2010}^{\mathrm{OMI}}$ is the average OMI column concentration from 2005 to 2010.

2.2 GlobeLand30 LUCC data

GlobeLand30 is a global surface coverage product with

30-m spatial resolution, provided by China's National Administration of Surveying, Mapping and Geoinformation (NASG). NASG researchers produced these products for two base years of 2000 and 2010, using techniques such as multi-source image optimization and refined extraction of land-cover type (Chen et al., 2014). With high spatial resolution and classification accuracy, GlobeLand30 provided more accurate land-cover change information for our study. Compared with other moderate-resolution land-cover data, GlobeLand30 can better reflect the reality that urban area in China has been increasing rapidly since the turn of the 21st century. Therefore, we used GlobeLand30 to extract land-cover change information.

2.3 Evaluating effects of LUCC on N deposition

The effects of LUCC on N deposition were calculated by eqs. (3) and eq. (4). Eq. (3) calculates the effect of LUCC on the change rate of N deposition. Based on its results, the total change of N deposition since a LUCC was calculated by eq. (4).

$$R_{i\to j}=\frac{\sum\dfrac{N_{i\to j}^{2010}-N_{i\to j}^{2000}}{N_{i\to j}^{2000}}}{n_{i\to j}}, \tag{3}$$

where i and j are land-cover types in 2000 and 2010, respectively. The subscript $i{\to}j$ represents a change of land-cover type from i to j in the period 2000 to 2010. $R_{i\to j}$ is the change rate of N deposition when the land-cover type changes from i to j. $N_{i\to j}^{2000}$ and $N_{i\to j}^{2010}$ is the N deposition of a certain grid cell in 2000 and 2010, respectively, with the land cover changing from i to j. $n_{i\to j}$ is the total number of grid cells whose land-cover type changed from i to j. When land-cover type changed from i to j, labelled as subscript $i{\to}j$, $R_{i\to j}$ represents the change rate of N deposition in the period 2000–2010. If the land-cover type i was unchanged over that period, labelled as subscript $i{\to}i$, $R_{i\to i}$ symbolizes the average N deposition change rate of land-cover type i, which is the background change of N deposition for i. Comparing $R_{i\to j}$ with $R_{i\to i}$ indicates how LUCC alters the rate of N deposition.

$$\begin{aligned} Ndep_{i\to j}^{d} &= (\overline{Ndep_{i\to j}^{2000}} \times R_{i\to j} \\ &\quad -\overline{Ndep_{i\to j}^{2000}} \times R_{i\to i}) \times S_{i\to j}. \end{aligned} \tag{4}$$

In the above equation, i and j are land-cover types in 2000 and 2010. $\overline{Ndep_{i\to j}^{2000}}$ is the average N deposition of grid cells whose land-cover type was i in 2000 and changed to j by 2010. $S_{i\to j}$ is the total area of land whose cover changed from i to j. $Ndep_{i\to j}^{d}$ is total change of N deposition rate owing to land-cover type change from i to j.

2.4 Simulation of N deposition effects on C budgets

The effects of N deposition on C budgets in China were simulated by the process-based IBIS model. IBIS was first developed by Foley et al. (1996). Subsequently, Liu et al. (2005) improved the representation of N cycling processes in IBIS. The accuracy of this IBIS model has been validated not only at individual flux tower scale but also at regional and global scales. After several years of development, IBIS has been used widely in the studies of C, water, and N cycles in China (Lu et al., 2012; Yuan et al., 2014; Zhu et al., 2012). Therefore, IBIS was suitable for simulating N deposition effects on C budgets in the present study.

The initialization data of IBIS mainly includes multi-year average meteorological data, vegetation data, soil data and elevation data, which were collected from the China Meteorological Administration's data sharing website (http://data.cma.cn/), 1:4000000 vegetation maps of China, 1:1000000 soil dataset of China and SRTM (Shuttle Radar Topography Mission) global DEM (digital elevation model) data. The driving datasets of the IBIS model are gridded monthly meteorology data, N deposition data and atmospheric CO_2 concentration. The driving meteorology data was also produced from meteorology site observation data collected from the China Meteorological Administration's data sharing website using the annuspline interpolation method. N deposition data were simulated in this study. Atmospheric CO_2 concentration was calculated using an exponential equation based on the observation of background atmospheric CO_2 concentrations at the Mauna Loa, Hawaii, United States, station from 1959 to 2004.

The IBIS model simulation is divided into three stages. The first stage is the model preheating stage. Initial data are used to preheat the pools of C and N in the IBIS model. The second stage is to simulate the C and N cycles in IBIS under the influence of the driving data. The aim of this stage is to ensure the accuracy of the C budget simulation in preparation for the next stage. In the third stage, two simulation scenarios are used to evaluate the effects of N deposition on the C budget. In one scenario, the N deposition level, was fixed at the year 2000. In another scenario, N deposition varied with time. Details about the three stages are listed in Table 1.

2.5 Assessing effects of N deposition change caused by LUCC on C budget

Due to LUCC, the effects of N deposition change on C budget come from two parts. One is the responses of net primary production (NPP) and net ecosystem production (NEP) to N deposition are changed after LUCC. The average effects of N deposition on the NPP and NEP of each land-cover type are calculated by eq. (5). The other is the increasing rate of N deposition changes since the LUCC can be calculated by eq. (3). In summary, the effects of N deposition change caused by LUCC on C budget are assessed by eq. (6).

Table 1 Basic setting of model simulation

Stage	Scenarios	Range	Climate data	N deposition
1		1901–1950	Multi-year average	Multi-year average
2		1951–2000	Monthly average	Extended data
3	N0	2000–2010	Monthly average	Fixed at 2000
	N1	2000–2010	Monthly average	Monthly average

$$E_{i\to i}^{NPP}=\frac{\sum\dfrac{NPP_{i\to i}^{N1}-NPP_{i\to i}^{N0}}{Ndep_{i\to i}^{2010}-Ndep_{i\to i}^{2000}}}{n_{i\to i}},\quad E_{i\to i}^{NEP}=\frac{\sum\dfrac{NEP_{i\to i}^{N1}-NEP_{i\to i}^{N0}}{Ndep_{i\to i}^{2010}-Ndep_{i\to i}^{2000}}}{n_{i\to i}}. \tag{5}$$

In eq. (5), i represents the land-cover type. The subscript $i\to j$ represents the cells where the land-cover type had not changed from 2000 to 2010. $E_{i\to i}^{NPP}$ and $E_{i\to i}^{NEP}$ are the average effects of N deposition on NPP and NEP in land-cover type i, respectively. $NPP_{i\to i}^{N1}$ and $NEP_{i\to i}^{N1}$ are the NPP and NEP under the N1 simulation scenario, respectively. $NPP_{i\to i}^{N0}$ and $NEP_{i\to i}^{N0}$ are the NPP and NEP under the N0 simulation scenario, respectively. $Ndep_{i\to i}^{2000}$ and $Ndep_{i\to i}^{2010}$ are the N deposition levels in 2000 and 2010, respectively. $n_{i\to i}$ is the total number of grid cells in which land-cover type was not changed.

$$\begin{aligned}NPP_{i\to j}^{d}&=(E_{j\to j}^{NPP}\times\overline{Ndep_{i\to j}^{2000}}\times R_{i\to j}\\&\quad-E_{i\to i}^{NPP}\times\overline{Ndep_{i\to j}^{2000}}\times R_{i\to i})\times S_{i\to j},\\NEP_{i\to j}^{d}&=(E_{j\to j}^{NEP}\times\overline{Ndep_{i\to j}^{2000}}\times R_{i\to j}\\&\quad-E_{i\to i}^{NEP}\times\overline{Ndep_{i\to j}^{2000}}\times R_{i\to i})\times S_{i\to j},\end{aligned} \tag{6}$$

where $NPP_{i\to j}^{d}$ and $NEP_{i\to j}^{d}$ are the effects of N deposition change caused by LUCC on NPP and NEP, respectively. $\overline{Ndep_{i\to j}^{2000}}$ is the average N deposition level in 2000 with land-cover type changing from $i\to j$. $R_{i\to j}$ is the change of N deposition rate when land-cover type change from i to j. $R_{i\to i}$ is the average change rate of N deposition when land-cover type is always i from 2000 to 2010. $S_{i\to j}$ is the total area of land cover whose type changed from i to j .

3. Results and discussion

3.1 N deposition rates calculated from NO_2 column data

N deposition rates were calculated from NO_2 column and gridded meteorology datasets from 2000 to 2010, using eq. (1). The calculated N deposition rates were validated by data from previous studies (Table 2). The estimated N deposition is close to the results of those studies. The simulated results had a higher accuracy for forests than for croplands. The reason is that N_4^+ deposition is the major form of N deposited in croplands, but NO_2 columns do not measure atmospheric N_4^+; instead, they mainly reflect nitrate. Although N_4^+ was considered in the MOZART model outputs used in eq. (2), N deposition in cropland was still underestimated. If the accuracy of NH_3 columns from space is improved, our calculations of N deposition over cropland might be more accurate. Generally, our estimation method is more suitable to the ecosystems that are less disturbed by human activity. The calculations gave less national average N deposition than the integration of observations from multiple sites. Because the observation sites were mainly in areas with substantial human activity, the aggregation of single-site observations to give regional estimates may have led to overestimation of actual N deposition. Therefore, our estimation method is better for large-scale N deposition estimation, because of the continuous and uniform spatiotemporal coverage of satellite data.

From 2000 to 2010, the average N deposition was 1.3 g N m^{-2} yr^{-1}, and the national total was 12.5 Tg N yr^{-1}. N deposition rates increased from 1.2 g N m^{-2} yr^{-1} in 2000 to 1.6 g N m^{-2} yr^{-1} in 2010, due to the intensifying human activity in the country. The average rate of increase was 0.35 Tg N yr^{-1}. The increase in N deposition is closely related to the rising consumption of fossil fuels and fertilizer (Figure 1b and c), which are the main sources of reactive N in the atmosphere over China (Gu et al., 2012).

Figure 1a shows that N deposition was high in eastern China and low in the west. Because of the relatively low reactive N emissions in western China, N deposition was only 0.2–0.5 g N m^{-2} yr^{-1}, nearly equal the natural background rate of N deposition. In the Northeast Plain, N deposition was 1–2 g N m^{-2} yr^{-1}. As reactive N emissions increased, N deposition increased from west to east. The North China Plain, Yangtze River Delta, and Sichuan Basin in eastern China had high N deposition, within the range of 3–4 g N m^{-2} yr^{-1}. In addition, in the eastern coastal areas and southwest, N deposition was < 1.5 g N m^{-2} yr^{-1}.

N deposition rates in industrially and agriculturally developed regions of southeast China have exceeded average levels in Europe and the United States. In industrial areas of the latter, the average N deposition rate is ~1 g N m^{-2} yr^{-1}. In Western Europe, the rate is 1–2 g N m^{-2} yr^{-1}. In industrial areas of India, the mean rate is 2 g N m^{-2} yr^{-1} (Reay et al.,

Table 2 Validation of N deposition rates calculated from NO_2 column data (g N m^{-2} yr^{-1})

ID	Location	Land cover	Time	This study			Previous study			Reference
				Avg.	max	Min	Avg.	max	min	
1	Yingtan, Jiangxi	Forest	2004–2005	1.2	1.95	1.06	0.97			Fan et al., 2007
2	North China pain	Crop	2003–2004	2.02	4.82	1.17	2.47	4.07	1.49	Zhang et al., 2006
3	South of Jilin Province	Crop and grass	2004	0.62	1.21	0.42	1			Li et al., 2010
4	Jiulong river, Fujian	Crop and forest	2004–2005	1.44	1.67	0.83	1.48			Chen et al., 2008
5	50 sites	Forest	1980–2009	1.56	5.08	0.15	2.08	7.1	0.28	Fang et al., 2011
6	China	All	2003	1.1			1.3			Lü and Tian, 2007
7	270 sites	All	2000s	1.3			2.1			Liu et al., 2013

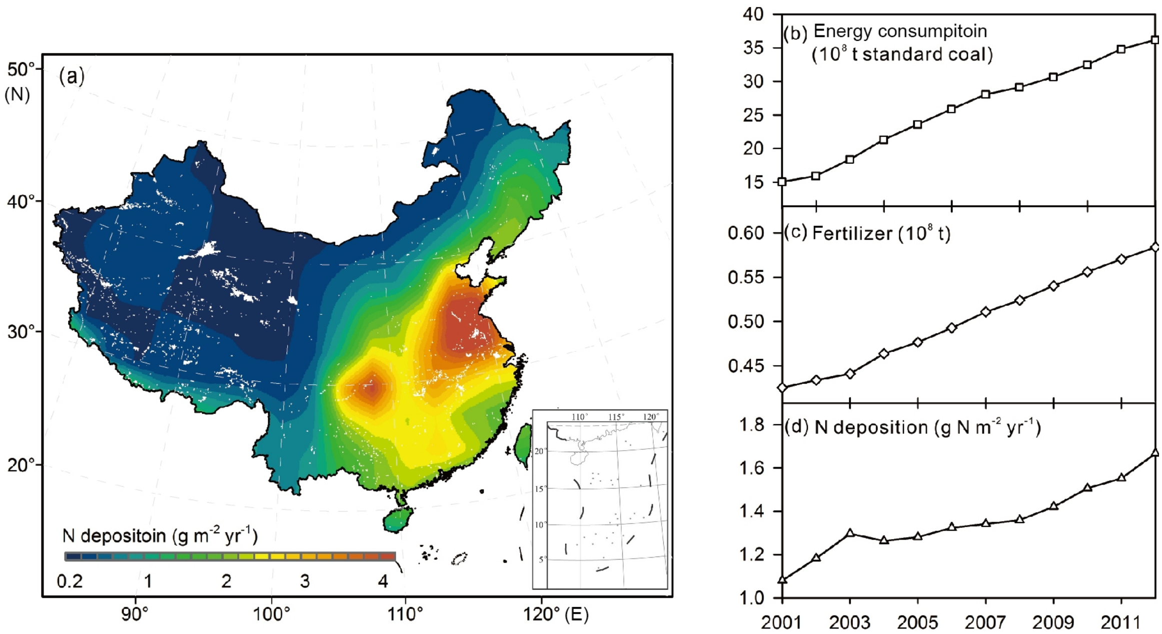

Figure 1 Multiyear average N deposition (2000–2009).

2008). Compared with the above areas, southeast China has become another region with a high rate of N deposition.

3.2 LUCC effects on N deposition

Land-cover changes between crop, grass, forest and urban areas occurred under the guidance of state policy in China since the beginning of the 21st century (Liu et al., 2014). The current situation of these major LUCC types was extracted from GlobeLand30 and is described in Table 3 and Figure 2.

LUCC can alter the properties of N deposition by changing features of the ground surface (turbulent diffusion, Brownian diffusion, and surface absorption) and reactive N emission (mainly NO_x and NH_3). In China, changes into forest have greatly affected N deposition. When forest changed into the other land-cover types, N deposition rates increased very fast, as shown in Figure 3. The change from forest to cropland increase the rate of N deposition to be higher than any of the other changes between land cover types. However, changes into forest slowed the rate of N deposition increase. For instance, the change of cropland to forest caused the largest decline of N deposition increase (Figure 3c). And when urban areas were changed into forest, the rate of N deposition increase was also slowed obviously (Figure 3d).

On a national scale, changes from forest to grassland and cropland increased total N deposition by 0.249 and 0.444 Gg N yr^{-1}, respectively. However, changes of cropland and grassland into forest slowed the rate of increase in N deposition, resulting in deposition decreases of 0.376 and 0.538 Gg N yr^{-1} (Figure 4). Other types of land-cover change had lesser effects than the four types mentioned above. The net effect of all LUCC was to reduce the increase of N deposition by 0.210 Gg N yr^{-1}.

3.3 Effects of N deposition change on C budget

IBIS-simulated C budgets were validated against earlier research results for various periods, as shown in Table 4. IBIS-simulated NPP is lower than most of those results, which can be explained by two factors. First, dynamics of the area fraction of vegetation types within grids of the IBIS model can

Table 3 Land-use transitions in China (10^4 ha)

		2010				Decline
		Forest	Grass	Crop	Urban	
2000	Forest	–	136.05	89.12	3.90	229.07
	Grass	127.93	–	31.35	4.41	163.69
	Crop	102.82	25.06	–	24.80	152.68
	Urban	3.22	1 .81	13.12	–	18.15
Increase		233.97	162.92	133.59	33.11	

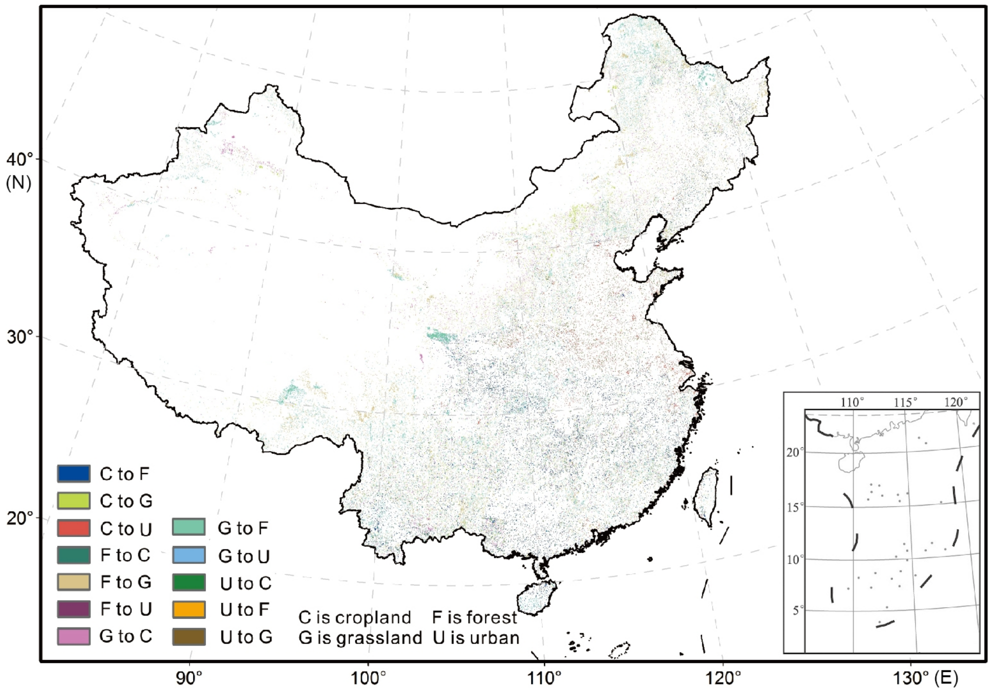

Figure 2 Major land-cover change in China. C, cropland; F, forest; G, grassland; U, urban. LUCC can be represented using these letters; e.g., forest change into cropland can be represented as F to C.

Table 4 Validation of IBIS-simulated NPP and NEP[a)]

System	Period	This study		Previous studies			Reference
		NPP	NEP	NPP	NEP	Method	
National avg.	1980–2002	–	70.2	–	173±39	Model	Piao et.al., 2009
National avg.	1995–1998	2.68	83.7	3.09	70	Model, RS	Cao et.al., 2003
National avg.	1981–2000	2.62	69.8	2.94	100	Model	Ji et.al., 2008
National avg.	2001	2.73	–	2.24	–	Model, RS	Feng et.al., 2007
Forest	1990–1999	1.08	87.4	1.13	189	Model	Ju et.al., 2007
Forest	1977–2003	–	70.4	–	75.2	CMB	Fang et.al., 2007
Forest	1990–2007	–	89.3	–	87.5	CMB	Pan et.al., 2011

a) Unit of NPP is Pg C yr^{-1}; that of NEP is Tg C yr^{-1} (Pg=10^{15}g, Tg=10^{12}g); CMB, carbon mass balance; RS, remote sensing.

make the simulated NPP low. Second, N limitation of the C budgets has not been considered in most modelling studies, but IBIS considers it explicitly. In summary, the IBIS-simulated NPP is still within acceptable ranges of the previous studies. Those studies have shown substantial uncertainties in NEP. Model-simulated results are generally greater than those derived using the C mass balance (CMB) method. The IBIS-simulated NEP is lower than other models' simulated NEP. One reason is that the NPP in IBIS is less than in other models. The other reason is that N control of biogeochemical cycling in IBIS makes soil respiration more reasonable than models without such control. Therefore, IBIS NEP is closer

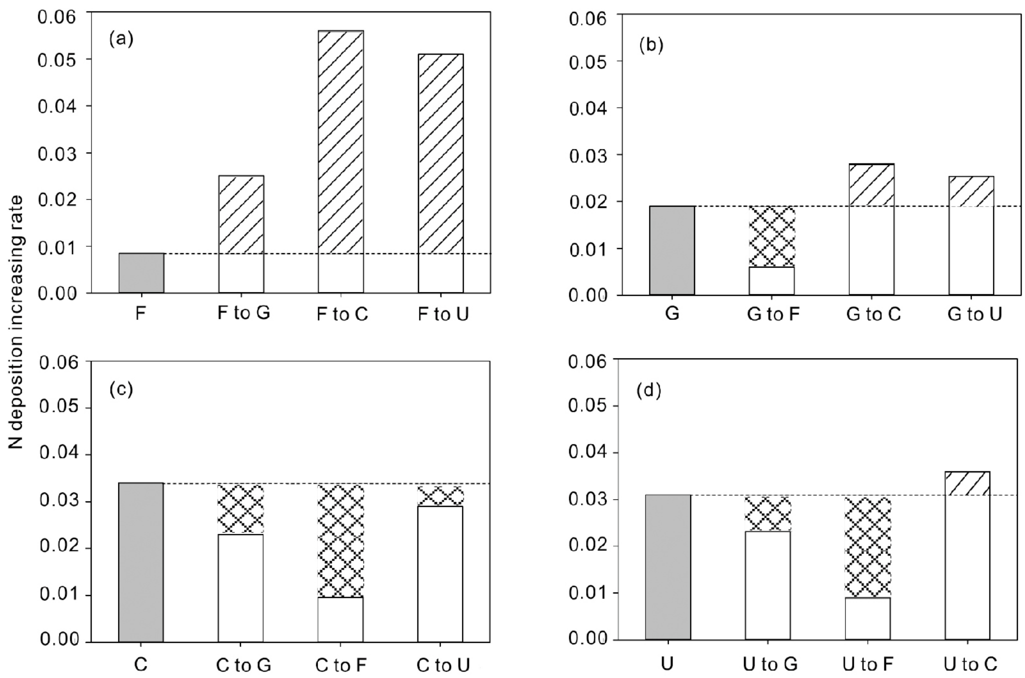

Figure 3 Changes in N deposition rate caused by LUCC. C, cropland; F, forest; G, grassland; U, urban. Grey bars are average rates of N deposition increase (background rate of N deposition increase); white bars are average rates of N deposition increase in areas of land-cover change; the bar filling with slashes and cross grids are increments and decrements in the rate of N deposition, respectively.

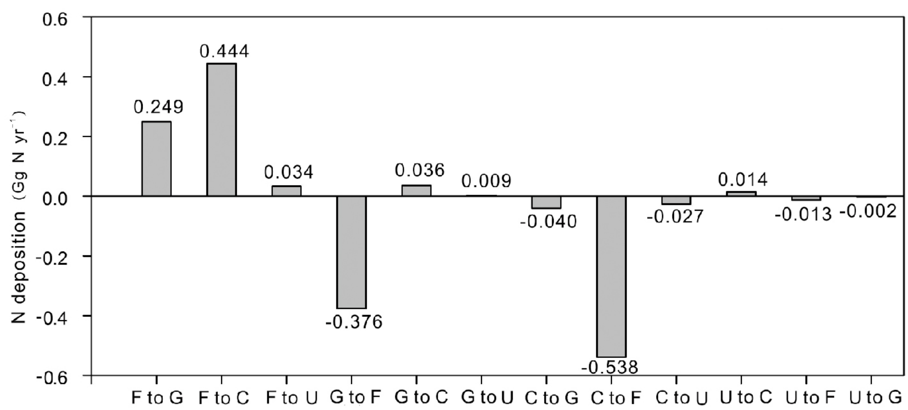

Figure 4 N deposition changes due to LUCC. C, cropland; F, forest; G, grassland; U, urban.

to CMB NEP, which is calculated from biomass survey data.

In Europe, the average NPP response to additional N deposition is 5–75 g C (g N)$^{-1}$ (de Vries et al., 2009). In China, the terrestrial ecosystem average NPP response to additional N deposition in the 1990s was 0–21 g C (g N)$^{-1}$. Average responses of NPP to additional N deposition in forests, grasslands and croplands in the early 21st century were respectively 35, 29 (25 in grassland and 33 in shrubland) and 4 g C (g N)$^{-1}$(Lu et al., 2012). Simulated responses of NPP to increasing N deposition in those land-use types were 42, 32 and 10 g C (g N)$^{-1}$, respectively. The national average from 2000 to 2010 was 25 g C (g N)$^{-1}$, close to the results of previous studies. The validation of NPP response to additional N deposition shows that the IBIS model can better simulate coupling effects between C and N, and was suitable for this study.

Increased N deposition raised NPP by 9.6 g C m^{-2} yr^{-1} on average, accounting for ~92.2 Tg C yr^{-1} of the national total. In most parts of China, NPP increases were < 0.01 kg C m^{-2} yr^{-1}. However, in the forests of southeast China and the Sichuan Basin, NPP response was clearly sensitive to N deposition (Figure 5a). The increased N deposition increased NEP by 4.6 g C m^{-2} yr^{-1} on average, or ~46.9Tg C yr^{-1} of the national total. The most positive effects of N deposition on NEP were in the forest areas of Zhejiang, Fujian, Sichuan, Hainan, and Daxing'anling (Figure 5b), with a rate of increase 0.05–0.08 kg C m^{-2} yr^{-1}. The negative effects of N deposition on NEP were widespread in the north-west and strongest in the southwest, where under increased N deposi-tion, enhanced C assimilation was outweighed by increased soil respiration. Studies have shown that LUCC has turned terrestrial ecosystems from weak C sources into weak C sinks (Ge et al., 2008). Our study indicated that N deposition has increased NPP and NEP, which has promoted the conversion of terrestrial ecosystems from C sources into C sinks.

In some areas, the highest N deposition did not induce strong responses of NPP and NEP. For example, in cropland, N deposition increased by 0.21 g N m^{-2} on average, the greatest increase among the land-cover types from 2000 to 2010. However, the responses of NPP and NEP to this deposition were only 9.80 and 2.93 g C (g N)$^{-1}$. Because cropland is an N-rich ecosystem, N input from its deposition cannot clearly augment NPP and NEP. Therefore, the responses of NPP and NEP to increasing N deposition in cropland were much weaker than in grassland and forest (Table 5). Because N deposition in grassland only increased by 0.04 g N m^{-2}, it did not enhance NPP and NEP much. A strong impact of N deposition on C budgets was found in forest, where the deposition increase was more obvious (0.16 g N m^{-2}) and N use efficiency was high (Table 5).

LUCC changed the N deposition rate of increase and affected the responses of NPP and NEP to additional N deposition (NPP/N_{dep} and NEP/N_{dep}), which were the two main influences on our results. According to the calculation in Table 5, when forest was changed into grassland and cropland, the increase of NPP and NEP from increased N deposition caused by LUCC was greater than the decrease of NPP and NEP from the effects of NPP/N_{dep} and NEP/N_{dep} change. Therefore, in such land-type transition, changes of N deposition from LUCC increased NPP and NEP. In another typical change, cropland to grassland and forest, although rates of N deposition increase were restrained, NPP and NEP still increased because of their heightened responses to N deposition (i.e., increases in NPP/N_{dep} and NEP/N_{dep}).

The net effect of N deposition changes caused by LUCC on total NPP and NEP was to reduce them by 0.7 and 0.4 Gg C yr^{-1}, respectively, from 2000 to 2010. Among various types of land-cover change, changes from grassland into forest and cropland reduced NPP and NEP most. Comprehensive effects of slower rates of N deposition increase and reduced responses of NPP and NEP to N deposition clearly decreased NPP and NEP in such change. Furthermore, this type of land-cover change made up the large part of the total

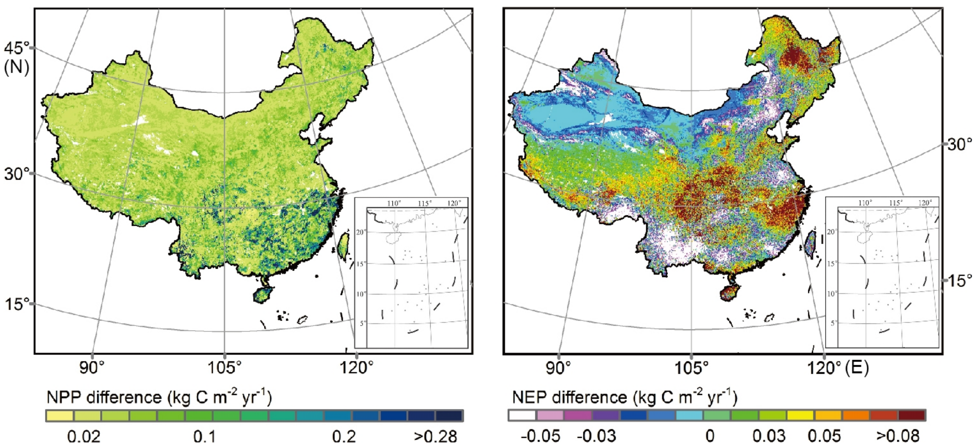

Figure 5 Simulated effects of N deposition on NPP and NEP (2000–2010).

Table 5 Effects of N deposition change caused by LUCC on C budget

Land cover	NPP/ N_{dep}	NEP/ N_{dep}	Land cover change	Average N_{dep} (2000)	Rate of N_{dep} increase		Total area of land cover change	Carbon budget			
					Initial land cover	Changed land cover		Average NPP	Average NEP	Total NPP	Total NEP
	eq. (5)	eq. (5)		$Ndep_{i\to j}^{2000}$	$R_{i\to i}$	$R_{i\to j}$	$S_{i\to j}$			eq. (6)	eq. (6)
	g C (g N)$^{-1}$			g N m^{-2} yr^{-1}			10^{10} m^2	g C m^{-2} yr^{-1}		10^{10} g C yr^{-1}	
Forest	41.88	12.75	Grass	1.11	0.0085	0.025	1.36	0.49	0.17	0.67	0.24
			Crop	1.10		0.056	0.85	0.21	0.06	0.18	0.05
Grass	32.03	10.58	Forest	2.26	0.0190	0.006	1.28	−0.81	−0.28	−1.03	−0.36
			Crop	1.29		0.028	0.31	−0.43	−0.15	−0.13	−0.05
Crop	9.80	2.93	Grass	1.47	0.0340	0.023	0.25	0.59	0.21	0.15	0.05
			Forest	2.09		0.009	1.03	0.09	0.03	0.09	0.03

LUCC area. Therefore, the change from grassland into forest and cropland was the major reason for NPP and NEP reduction. Compared with the total effects of N deposition on NPP and NEP, N deposition changes caused by LUCC had a limited aggregate effect on the C budget.

4. Conclusions

In this study, N deposition calculated from remotely sensed NO_2 column data and GlobeLand30 datasets was used to evaluate the effects of N deposition caused by LUCC on the C budget in China, with the aid of the IBIS model. The study showed that LUCC decreased N deposition by 0.21 Gg N yr^{-1}, which was mainly caused by changes of cropland and grassland into forest. LUCC also changed the sensitivity of the C budget to N deposition. Generally, the influence of LUCC on N deposition reduced NPP and NEP by 0.7 and 0.4 Gg C yr^{-1}, respectively. Among all typical LUCC, the change from grassland into forest and cropland was the major factor that reduced NPP and NEP.

Acknowledgements *This work was supported by the National Natural Science Foundation of China (Grant No. 41501212), the National Natural Science Foundation of China Major Program (Grant No. 41171324), Funds for Ph.D. Education (Grant No. 20110091110028), and the MOST Fundamental Research Project (Grant No. 2005DKA32306).*

References

Cao M, Prince S D, Li K, Tao B, Small J, Shao X. 2003. Response of terrestrial carbon uptake to climate interannual variability in China. Glob Change Biol, 9: 536–546

Chen J, Chen J, Miao P, Cao X, Chen L, Chen X, Peng S, Han G, Zhang H, He C, Wu H, Wu H, Lu M. 2014. Concepts and key techniques for 30m global land cover mapping (in Chinese). Acta Geo Et Carto Sin, 43: 551–557

Chen N, Hong H, Zhang L. 2008. Wet deposition of atmospheric nitrogen in Jiulong river watershed. Environ Sci, 29: 38–46

Cornell S E, Jickells T D, Cape J N, Rowland A P, Duce R A. 2003. Organic nitrogen deposition on land and coastal environments: A review of methods and data. Atmos Environ, 37: 2173–2191

de Vries W, Solberg S, Dobbertin M, Sterba H, Laubhann D, van Oijen M, Evans C, Gundersen P, Kros J, Wamelink G W W, Reinds G J, Sutton M A. 2009. The impact of nitrogen deposition on carbon sequestration by European forests and heathlands. For Ecol Manage, 258: 1814–1823

Dentener F, Drevet J, Lamarque J F, Bey I, Eickhout B, Fiore A M, Hauglustaine D, Horowitz L W, Krol M, Kulshrestha U C, Lawrence M, Galy-Lacaux C, Rast S, Shindell D, Stevenson D, Van Noije T, Atherton C, Bell N, Bergman D, Butler T, Cofala J, Collins B, Doherty R, Ellingsen K, Galloway J, Gauss M, Montanaro V, Müller J F, Pitari G, Rodriguez J, Sanderson M, Solmon F, Strahan S, Schultz M, Sudo K, Szopa S, Wild O. 2006. Nitrogen and sulfur deposition on regional and global scales: A multimodel evaluation. Glob Biogeochem Cycle, 20: GB4003

Fan J, Hu Z, Zhuang Y, Zhou J, Wang T, Liu C. 2007. Observation of atmospheric nitrogen deposition into forestland (in Chinese). China Environ Sci, 27: 7–9

Fang J Y, Guo Z D, Piao S L, Chen A P. 2007. Terrestrial vegetation carbon sinks in China, 1981–2000. Sci China Ser D-Earth Sci, 50: 1341–1350

Fang Y, Gundersen P, Vogt R D, Koba K, Chen F, Chen X Y, Yoh M. 2011. Atmospheric deposition and leaching of nitrogen in Chinese forest ecosystems. J For Res, 16: 341–350

Foley J A, Prentice I C, Ramankutty N, Levis S, Pollard D, Sitch S, Haxeltine A. 1996. An integrated biosphere model of land surface processes, terrestrial carbon balance, and vegetation dynamics. Glob Biogeochem Cycle, 10: 603–628

Feng X, Liu G, Chen J M, Chen M, Liu J, Ju W M, Sun R, Zhou W. 2007. Net primary productivity of China's terrestrial ecosystems from a process model driven by remote sensing. J Environ Manage, 85: 563–573

Ge Q S, Dai J H, He F N, Pan Y, Wang M M. 2008. Land use changes and their relations with carbon cycles over the past 300 a in China. Sci China Ser D-Earth Sci, 51: 871–884

Gu B, Ge Y, Ren Y, Xu B, Luo W, Jiang H, Gu B, Chang J. 2012. Atmospheric reactive nitrogen in China: Sources, recent trends, and damage costs. Environ Sci Technol, 46: 9420–9427

Gu B J, Yang G F, Luo W D, Du Y Y, Ge Y, Chang J. 2013. Rapid growth of industrial nitrogen fluxes in China: Driving forces and consequences. Sci China Earth Sci, 56: 662–670

Ji J J, Huang M, Li K R. 2008. Prediction of carbon exchanges between China terrestrial ecosystem and atmosphere in 21st century. Sci China Ser D-Earth Sci, 51: 885–898

Ju W M, Chen J M, Harvey D, Wang S. 2007. Future carbon balance of China's forests under climate change and increasing CO_2. J Environ Manage, 85: 538–562

Li B, Liu Y, Yao Y, Fang F, Zhang Z, Xu X. 2010. Element flux and sources from atmospheric bulk deposition in Western Jilin Province (in Chinese). J Jilin Univ-Earth Sci Ed, 40: 176–182

Lü C, Tian H. 2007. Spatial and temporal patterns of nitrogen deposition in China: Synthesis of observational data. J Geophys Res, 112: D22S05

Lü C, Tian H. 2014. Half-century nitrogen deposition increase across China: A gridded time-series data set for regional environmental assessments. Atmos Environ, 97: 68–74

Lü C, Tian H, Liu M, Ren W, Xu X, Chen G, Zhang C. 2012. Effect of nitrogen deposition on China's terrestrial carbon uptake in the context of multi-factor environmental changes. Ecol Appl, 22: 53–75

Law B. 2013. Biogeochemistry: Nitrogen deposition and forest carbon. Nature, 496: 307–308

Liu J, Kuang W, Zhang Z, Xu X, Qin Y, Ning J, Zhou W, Zhang S, Li R, Yan C, Wu S, Shi X, Jiang N, Yu D, Pan X, Chi W. 2014. Spatiotemporal characteristics, patterns, and causes of land-use changes in China since the late 1980s. J Geogr Sci, 24: 195–210

Liu J, Price D T, Chen J M. 2005. Nitrogen controls on ecosystem carbon sequestration: A model implementation and application to Saskatchewan, Canada. Ecol Model, 186: 178–195

Liu X, Zhang Y, Han W, Tang A, Shen J, Cui Z, Vitousek P, Erisman J W, Goulding K, Christie P, Fangmeier A, Zhang F. 2013. Enhanced nitrogen deposition over China. Nature, 494: 459–462

Lu X, Jiang H, Zhang X, Liu J, Zhang Z, Jin J X, Wang Y, Xu J, Cheng M. 2013. Estimated global nitrogen deposition using NO_2 column density. Int J Remote Sens, 34: 8893–8906

Lu X, Jiang H, liu J, Zhou G, Zhu Q, Peng C, Wei X, Chang J, Liu S, Liu S, Zhang Z, Wang K, Zhang X, Solomon A. 2012. Spatial and temporal variability of nitrogen deposition and its impacts on the carbon budget of China. Proc Environ Sci, 13: 1997–2030

Luo Y, Su B, Currie W S, Dukes J S, Finzi A, Hartwig U, Hungate B, Mc Murtrie R E, Oren R, Parton W J, Pataki D E, Shaw M R, Zak D R, Field C B. 2004. Progressive nitrogen limitation of ecosystem responses to rising atmospheric carbon dioxide. Bioscience, 54: 731–739

Ma S, Yang X, Li Z. 2012. An approach of estimating the atmospheric deposition of nitrogen to the coastal water using GOME-2 satellite data (in Chinese). Mar Environ Sci, 31: 272–276

Norby R J, Warren J M, Iversen C M, Medlyn B E, McMurtrie R E. 2010.

CO_2 enhancement of forest productivity constrained by limited nitrogen availability. Proc Natl Acad Sci USA, 107: 19368–19373

Ouyang Y, Wang T, Zhang Y, Hu Z, Xu C. 2003. A method calculating dry deposition velocity of air pollutants and its application (in Chinese). J Nanjing Institute of Meteorol, 26: 210–218

Pan Y, Birdsey R A, Fang J, Houghton R, Kauppi P E, Kurz W A, Phillips O L, Shvidenko A, Lewis S L, Canadell J G, Ciais P, Jackson R B, Pacala S W, McGuire A D, Piao S, Rautiainen A, Sitch S, Hayes D. 2011. A large and persistent carbon sink in the world's forests. Science, 333: 988–993

Piao S, Fang J, Ciais P, Peylin P, Huang Y, Sitch S, Wang T. 2009. The carbon balance of terrestrial ecosystems in China. Nature, 458: 1009–1013

Reay D S, Dentener F, Smith P, Grace J, Feely R A. 2008. Global nitrogen deposition and carbon sinks. Nat Geosci, 1: 430–437

Seinfeld J H, Pandis S N. 2012. Atmospheric chemistry and physics: From air pollution to climate change. Physics Today

Yuan W, Liu D, Dong W, Liu S, Zhou G, Yu G, Zhao T, Feng J, Ma Z, Chen J, Chen Y, Chen S, Han S, Huang J, Li L, Liu H, Liu S, Ma M, Wang Y, Xia J, Xu W, Zhang Q, Zhao X, Zhao L. 2014. Multiyear precipitation reduction strongly decreases carbon uptake over northern China. J Geophys Res Biogeosci, 119: 881–896

Zhang Q, Wang Y P, Matear R J, Pitman A J, Dai Y J. 2014. Nitrogen and phosphorous limitations significantly reduce future allowable CO_2 emissions. Geophys Res Lett, 41: 632–637

Zhang Y, Liu X, Zhang F, Ju X, Zou G, Hu K. 2006. Spatial and temporal variation of atmospheric nitrogen deposition in the North China Plain. Acta Ecol Sin, 26: 1633–1638

Zhu Q, Jiang H, Peng C, Liu J, Fang X, Wei X, Liu S, Zhou G. 2012. Effects of future climate change, CO_2 enrichment, and vegetation structure variation on hydrological processes in China. Glob Planet Change, 80-81: 123–135